A Review and Application of the Finite-Difference Time-Domain Algorithm Applied to the Schrödinger Equation

J. R. Nagel

University of Utah
Department of Electrical and Computer Engineering
Salt Lake City, Utah, USA
james.nagel@utah.edu

Abstract – This paper contains a review of the FDTD algorithm as applied to the time-dependent Schrödinger equation, and the basic update equations are derived in their standard form. A simple absorbing boundary condition is formulated and shown to be effective with narrowband wave functions. The stability criterion is derived from a simple, novel perspective and found to give better efficiency than earlier attempts. Finally, the idea of probability current is introduced for the first time and shown how it can be used to radiate new probability into a simulation domain. This removes the need to define an initial-valued wave function, and the concept is demonstrated by measuring the transmission coefficient through a potential barrier.

I. INTRODUCTION

Most electrical engineers are already familiar with the Finite-Difference Time-Domain (FDTD) algorithm as a popular tool for simulating the progression of time-dependent Maxwell equations. However, as the push for miniaturization brings us closer to the realm of nanoscale devices, Maxwell's equations can no longer be relied upon to provide useful insight. Nanoscale integrated circuits, quantum computers, and solid-state devices are just a few of the emerging electronic technologies that cannot be understood using classical electromagnetic theory. Instead, we must delve into the realm of quantum mechanics, where the laws of physics are more correctly governed by the Schrödinger equation. It will therefore be useful for electrical engineers to gain a deeper understanding of the Schrödinger equation, as well as develop a rigorous set of software tools for simulating the time-development of complex quantum systems. In particular, FDTD is a well-suited tool for this task, and can be easily modified for quantum simulation.

The first attempt to create a working FDTD algorithm for the Schrödinger equation was published by Goldberg et. al. in 1967 [1], but remained relatively obscure for many years. After 1990, the topic began to receive greater attention in the literature [2–4], most of which has been based on the Crank-Nicholson scheme. In 2004, Soriano et. al. rigorously formulated a more efficient FDTD algorithm and dubbed it "FDTD-Q" in order to distinguish its application for quantum systems [5]. Meanwhile, quantum FDTD has already been used for many practical applications such as numerical simulation of quantum dots [6] and the time-progression of quantum logic gates [7].

Despite the recent activities surrounding FDTD-Q, the number of publications on the topic are a tiny fraction of what has been devoted to Maxwell's equations. Furthermore, many subtle nuances inherent to the Schrödinger equation tend to emerge when an FDTD-Q is applied. Thus, the goal of this paper is to review the basic FDTD-Q algorithm and to introduce new topics for future research. It is assumed that the reader is reasonably familiar with the Maxwellian FDTD, and so little time needs to be spent on the minor details and terminology. It is further assumed that the reader is at least familiar with basic quantum theory, though the more important expressions are reviewed in section II. For a more complete study of quantum mechanics, the reader is referred to [8] and [9].

The basic update equations of the FDTD-Q algorithm are derived in section III, and the information here is similar to what can be found in [5]. The issue of numerical stability is discussed in section IV, and the critical time step is derived from a unique, and hopefully more intuitive, perspective from that given by [10]. A Mur absorbing boundary condition is studied in section V, after which a simple example of quantum tunneling is simulated in section VI. Finally, we will introduce the novel concept of probability currents in section VII and show how they can be used to inject plane waves into a quantum simulation domain.

II. BACKGROUND

Just as Maxwell's equations are fundamental to all of electromagnetics, the Schrödinger equation is fundamental to all of quantum mechanics. The three-dimensional, time-dependent Schrödinger equation is therefore given

as [8],

$$j\hbar\frac{\partial\psi(\mathbf{r},t)}{\partial t} = -\frac{\hbar^2}{2m}\nabla^2\psi(\mathbf{r},t) + V(\mathbf{r})\psi(\mathbf{r},t) \qquad (1)$$

where $\psi(\mathbf{r},t)$ is the wave function at position $\mathbf{r}$ and time t, $V(\mathbf{r})$ is the potential function, m is the particle mass, and $\hbar$ is the reduced Planck's constant. Although $\psi(\mathbf{r},t)$ is not a physically measurable quantity, it is necessary in order to compute the function $\rho(\mathbf{r},t)$ defined by,

$$\rho(\mathbf{r},t) = \psi^*(\mathbf{r},t)\psi(\mathbf{r},t) = |\psi(\mathbf{r},t)|^2 \ . \qquad (2)$$

The interpretation of ρ is that of a time-varying probability density function (pdf) for the position of the particle. Thus, the total probability P of finding the particle in some volume V is found by integrating ρ over all points within that volume, [8]

$$P = \int_V \rho(\mathbf{r},t)d\mathbf{r} \ . \qquad (3)$$

Due to this probabilistic interpretation, the wave function must be normalized so that integration of ρ over all space produces a value of 1. It also serves to emphasize how the wave-particle duality of nature is really only an expression of how the positional pdf of a particle is governed by a wave-like equation.

The wavenumber amplitude $\phi(\mathbf{k})$ is defined by the Fourier transform of ψ at $t = 0$. In three dimensions, this is given by, [8]

$$\phi(\mathbf{k}) = \frac{1}{(2\pi)^{3/2}}\int_{-\infty}^{+\infty}\psi(\mathbf{r},0)e^{-j\mathbf{k}\cdot\mathbf{r}}d\mathbf{r} \qquad (4)$$

where $\mathbf{k}$ is the wave-vector. In particular, $\mathbf{k}$ is important because it tells us the particle's momentum, which is given by $\mathbf{p} = \hbar\mathbf{k}$. The function ϕ, like ψ, is not directly observable, but is only used to compute the pdf defined by $|\phi(\mathbf{k})|^2$. This quantity represents the probability density of detecting the wave-vector $\mathbf{k}$ after a given experiment. Thus, like before, the total probability P_k of detecting some wave-vector (or equivalently, some momentum) within the volume V_k (in k-space) is found by, [8]

$$P_k = \int_{V_k}|\phi(\mathbf{k})|^2\,d\mathbf{k} \ . \qquad (5)$$

From this interpretation, it is clear that the Heisenberg uncertainty principle is merely a result of the Fourier relationship between probabilities in position-space and momentum-space. In other words, any restriction of variance within one domain will inevitably increase variance within the other.

III. UPDATE EQUATIONS

This next section parallels the derivations found in [4, 5], but with more explicit detail and clarification. We begin by noting that complex-valued arithmetic can be numerically costly, so it is helpful to first break up the wave function into real and imaginary components such that,

$$\psi(\mathbf{r},t) = \psi_R(\mathbf{r},t) + j\ \psi_I(\mathbf{r},t) \ . \qquad (6)$$

This step allows us to treat each component separately and perform only real-valued computations with each function. Plugging the real and imaginary components back into the Schrödinger equation thus produces two coupled partial differential equations of the form,

$$\hbar\frac{\partial\psi_R(\mathbf{r},t)}{\partial t} = -\frac{\hbar^2}{2m}\nabla^2\psi_I(\mathbf{r},t) + V(\mathbf{r})\psi_I(\mathbf{r},t) \qquad (7)$$

$$\hbar\frac{\partial\psi_I(\mathbf{r},t)}{\partial t} = +\frac{\hbar^2}{2m}\nabla^2\psi_R(\mathbf{r},t) - V(\mathbf{r})\psi_R(\mathbf{r},t) \qquad (8)$$

The next step is to define a mesh that discretely samples grid points in space and time. Using the standard FDTD notation for grid spacings of Δx, Δy, Δz, and time spacings of Δt, this gives,

$$x_i = i\Delta x \qquad (9)$$

$$y_j = j\Delta y \ , \qquad (10)$$

$$z_k = k\Delta z \ , \qquad (11)$$

$$t_n = n\Delta t \ . \qquad (12)$$

Note that in this context, j is not to be confused with the imaginary unit $\sqrt{-1}$ as implied by equation (1), nor is k to be confused with the particle wavenumber. We next define a short-hand notation for the wave function evaluated at the mesh points. This is given by,

$$\psi_R(x_i,y_j,z_k,t_n) = \psi_R^n(i,j,k) \qquad (13)$$

$$\psi_I(x_i,y_j,z_k,t_n) = \psi_I^n(i,j,k) \ . \qquad (14)$$

With the wave function sampled on a discrete grid, the derivatives will now be approximated by using finite-differences. For convenience, it helps to define the imaginary part of the wave function to exist at half-step time intervals from the real part. This is analogous to the way E-fields and H-fields are placed at half-step intervals in conventional FDTD because it facilitates the use of the central-difference method for the time derivatives. Thus, the time derivatives on the real- and imaginary-valued wave functions are approximated by,

$$\frac{\partial}{\partial t}\psi_R^{n+1/2}(i,j,k) \approx \frac{\psi_R^{n+1}(i,j,k) - \psi_R^n(i,j,k)}{\Delta t} \qquad (15)$$

$$\frac{\partial}{\partial t}\psi_I^n(i,j,k) \approx \frac{\psi_I^{n+1/2}(i,j,k) - \psi_I^{n-1/2}(i,j,k)}{\Delta t} \ . \qquad (16)$$

Similarly, we apply a central-difference on the spatial derivative to obtain the well-known approximation to the second-partial, given by,

$$\frac{\partial^2}{\partial x^2}\psi_R^n(i,j,k) \approx \frac{\psi_R^n(i+1,j,k) - 2\psi_R^n(i,j,k) + \psi_R^n(i-1,j,k)}{\Delta x^2} \qquad (17)$$

with a similar expression for all other spatial derivatives. Plugging these approximations back into equations (7) and (8) and solving for the update equations then gives the formulation as given by [5], which is,

$$\begin{aligned}\psi_R^{n+1}(i,j,k) &= \psi_R^n(i,j,k) \\ &- c_x\left[\psi_I^{n+1/2}(i+1,j,k) - 2\,\psi_I^{n+1/2}(i,j,k)\right. \\ &\qquad \left. + \psi_I^{n+1/2}(i-1,j,k)\right] \\ &- c_y\left[\psi_I^{n+1/2}(i,j+1,k) - 2\,\psi_I^{n+1/2}(i,j,k)\right. \\ &\qquad \left. + \psi_I^{n+1/2}(i,j-1,k)\right] \\ &- c_z\left[\psi_I^{n+1/2}(i,j,k+1) - 2\,\psi_I^{n+1/2}(i,j,k)\right. \\ &\qquad \left. + \psi_I^{n+1/2}(i,j,k-1)\right] \\ &+ c_v V(i,j,k)\psi_I^{n+1/2}(i,j,k)\end{aligned} \tag{18}$$

for the real part, and

$$\begin{aligned}\psi_I^{n+1/2}(i,j,k) &= \psi_I^{n-1/2}(i,j,k) \\ &+ c_x\left[\psi_R^n(i+1,j,k) - 2\psi_R^n(i,j,k) + \psi_R^n(i-1,j,k)\right] \\ &+ c_y\left[\psi_R^n(i,j+1,k) - 2\psi_R^n(i,j,k) + \psi_R^n(i,j-1,k)\right] \\ &+ c_z\left[\psi_R^n(i,j,k+1) - 2\psi_R^n(i,j,k) + \psi_R^n(i,j,k-1)\right] \\ &- c_v\; V(i,j,k)\psi_R^n(i,j,k)\;,\end{aligned} \tag{19}$$

for the imaginary part. The constant coefficients are given by,

$$c_x = \frac{\hbar\Delta t}{2m\Delta x^2} \tag{20}$$

$$c_y = \frac{\hbar\Delta t}{2m\Delta y^2}\;, \tag{21}$$

$$c_z = \frac{\hbar\Delta t}{2m\Delta z^2}\;, \tag{22}$$

$$c_v = \frac{\Delta t}{\hbar}\;. \tag{23}$$

From this point on, FDTD-Q is performed exactly the same as the Maxwellian FDTD. That is, an iterative loop solves for the state of the system at incremental time steps and "leap-frogs" between the real and imaginary components. Between each increment, the appropriate boundary conditions are applied.

It is interesting to compare the similarities between the Schrödinger and Maxwellian FDTD algorithms. For example, the real and imaginary wave functions are somewhat analogous to the electric and magnetic fields in the way they couple together in space and time. However, because of the second-order spatial derivatives, the real and imaginary wave functions can both exist at the same spatial grid point. Compare this with the Maxwellian FDTD, where the first-order derivatives require the electric and magnetic field stencils to be defined at half-step increments from each other in both space and time.

IV. STABILITY

The critical time step for stable FDTD-Q simulation was first derived by Soriano et. al. in 2004 by using an argument based on the "growth factor" of the wave function eigenvalues [5]. In 2005, Dai et. al. re-derived the stability criterion from the perspective of accumulated numerical error, and arrived at a similar, but more correct, solution [10]. This next section offers a third derivation that simply preserves the natural bounds of the wave function, and provides a more complete result than either [5] or [10]. For simplicity, the derivation is limited to one dimension and then briefly extended to three.

Suppose the potential function is a constant value such that $V(x) = V_0$. Solutions to the Schrödinger equation then take on the form of free particles with wave functions given by,

$$\psi(x,t) = \alpha_1 e^{j(kx-\omega t)} + \alpha_2 e^{j(kx+\omega t)} \tag{24}$$

where k is the particle wavenumber and ω is the angular frequency. Without any loss of generality, consider the simple case of a free particle traveling to the right where $\alpha_1 = 1$ and $\alpha_2 = 0$. The real and imaginary components are then simply,

$$\psi_R(x,t) = \cos(kx-\omega t) \tag{25}$$

$$\psi_I(x,t) = \sin(kx-\omega t)\;. \tag{26}$$

In terms of the FDTD stencil, these can be written as,

$$\psi_R^n(i) = \cos(ki\Delta x - \omega n\Delta t)\;, \tag{27}$$

$$\psi_I^n(i) = \sin(ki\Delta x - \omega n\Delta t)\;. \tag{28}$$

For convenience, let us now define $A = ki\Delta x - \omega n\Delta t$ so that,

$$\psi_R^n(i) = \cos(A) \tag{29}$$

$$\psi_I^n(i) = \sin(A)\;. \tag{30}$$

Furthermore, define the constants $B = k\Delta x$ and $C = \omega\Delta t$ so that,

$$\psi_R^{n+1}(i) = \cos(A-C) \tag{31}$$

$$\psi_I^{n+1/2}(i) = \sin(A-C/2)\;, \tag{32}$$

$$\psi_I^{n+1/2}(i+1) = \sin(A+B-C/2)\;, \tag{33}$$

$$\psi_I^{n+1/2}(i-1) = \sin(A-B-C/2)\;. \tag{34}$$

Next, substitute equations (29) to (34) back into equation (18) to find,

$$\begin{aligned}\cos(A-C) = &- c_x\left[\sin(A+B-C/2)\right. \\ &\quad - 2\sin(A-C/2) \\ &\quad \left. + \sin(A-B-C/2)\right] \\ &+ c_v V_0 \sin(A-C/2) + \cos(A)\;.\end{aligned} \tag{35}$$

The importance of equation (35) is that it places constraints on the available choices for c_x and c_v. If these

constants are not properly defined, then equation (35) can not be satisfied with real values for A, B, or C. As a result, numerical error quickly accumulates and the wave function increases without bound.

In order to maintain a stable simulation, it is necessary to choose the constants c_x and c_v such that equation (35) is satisfied by only real values of A, B, and C. The simplest way to do this is by choosing a time step Δt that prevents the right-hand side from ever exceeding the natural bounds of the left-hand side. In other words, we must enforce the condition that,

$$-1 \leq \cos(A - C) \leq 1 \ . \tag{36}$$

After applying this restriction to the right-hand side of equation (35), we find that c_x and c_v are limited by the extreme values of their multiplicative factors. For the positive bound of equation (36), this leads us to the expression,

$$4c_x + c_v V_0 \leq 2 \tag{37}$$

or equivalently

$$\frac{2\hbar\Delta t}{m\Delta x^2} + \frac{\Delta t V_0}{\hbar} \leq 2 \ . \tag{38}$$

Finally, solve for Δt to find,

$$\Delta t \leq \frac{\hbar}{\frac{\hbar^2}{m\Delta x^2} + \frac{V_0}{2}} \ . \tag{39}$$

The upper bound on Δt is called the *critical time step*, Δt_c, and represents the maximum allowable time increment that will maintain a stable simulation [5]. It is also the same result that is found by exploring the lower bound of equation (36) instead of the upper.

In the event that $V(x)$ is not a constant value, then equation (39) is still true for sectionally constant potentials, even if those potentials are only one grid point in size. As a result, every point in the domain essentially has its own limit for Δt, and a stable simulation is guaranteed only by ensuring that equation (39) is satisfied over all points within the simulation. Thus, the maximum allowable time step over a varying potential region $V(x)$ is found by,

$$\Delta t_c = \arg\min_x \left[\frac{\hbar}{\frac{\hbar^2}{m\Delta x^2} + \frac{V(x)}{2}} \right] \ . \tag{40}$$

If one follows the above derivation in three dimensions, it is straightforward to show that equation (37) will be rewritten into,

$$4(c_x + c_y + c_z) + c_v V(\mathbf{r}) \leq 2 \tag{41}$$

solving for the critical time step therefore yields,

$$\Delta t = \arg\min_{\mathbf{r}} \left[\frac{\hbar}{\frac{\hbar^2}{m}\left(\frac{1}{\Delta x^2} + \frac{1}{\Delta y^2} + \frac{1}{\Delta z^2}\right) + \frac{V(\mathbf{r})}{2}} \right] \ . \tag{42}$$

For comparison, the expression in equation (42) is nearly identical to that given by [5], except there is now a factor of $1/2$ which divides V in the denominator. This can make a significant difference for simulations where V is large in comparison to $\hbar^2/m\Delta x^2$.

The result in equation (42) is also similar to that given by Dai et. al. in [10], except for two key differences. First is the argument that the inequality of equation (42) should be limited to a less-than relation ($<$), and that inclusion of the upper bound does not necessarily guarantee stability. Fortunately, numerical truncation within a computer's memory will always set Δt to some value slightly smaller than its exact mathematical assignment. As a result, there is little practical difference in distinguishing between the ($<$) and ($\leq$) relations.

The second key difference in [10] is a replacement of $V(\mathbf{r})$ with $|V(\mathbf{r})|$, that is, all potentials are treated as positive values. For the case of a positive-definite V, this makes no difference and the two formulations are equivalent. However, for the case of negative potentials, Δt_c actually gets larger, and therefore does not influence the minimum time step over a simulation domain. So even though the formulation in [10] is certainly guaranteed to be stable, it does not necessarily provide one with the maximum stable value.

Interestingly, the critical time step seems to approach infinity as $V/2 \to -\hbar^2/m\Delta x^2$ and stable simulation is easily demonstrated for relatively large values of Δt_c. Indeed, it may even be possible to exploit this effect for faster quantum simulations. It remains unclear, however, what sort of trade-offs one incurs by pushing the limits of very large time steps in a domain of all-negative potentials. Experiments also demonstrate that for $V < -\hbar^2/m\Delta x^2$, the expression in equation (42) no longer provides stability, while the formulation in [10] still remains valid. Such behavior has yet to be fully analyzed, and a general expression for the maximum stable time step over all possible V remains unknown.

V. ABSORBING BOUNDARY CONDITIONS (ABCS)

Because of the nonlinear dispersion relation that arises from the Schrödinger equation, absorbing boundary conditions (ABCs) can be difficult to implement. The problem was first addressed by Shibata in 1991 [2], and then expanded upon by Kuska in 1992 [3]. Both solutions worked by devising a linear approximation to the dispersion relation and then formulating a corresponding partial differential equation to enforce at the boundaries. The problem was further addressed and formalized by Arnold et. al. [11], and has even been expanded by others to include the nonlinear Schrödinger equation [12]. To date, however, all of these formulations have been based on the Crank-Nicholson discritization, and none have been demonstrated in the FDTD-Q formulation of equations

(18) and (19). Therefore, this next section will introduce a simple ABC that is compatible with FDTD-Q.

The simplest ABC is the first-order Mur condition, which enforces a one-way wave equation at the boundaries. For a plane-wave traveling to the right in one dimension, this is given by, [13]

$$\frac{\partial}{\partial x}\psi(x,t) = -\frac{1}{v_p}\frac{\partial}{\partial t}\psi(x,t) \tag{43}$$

where v_p is the phase velocity of the wave impinging at the boundary. As an example, we will consider the rightmost boundary where $i = L$, though the end result is perfectly analogous at all other boundaries.

Solving for the update equations at the far-right grid point gives the familiar formulation, [13]

$$\psi_R^{n+1}(L) = \psi_R^n(L-1) + r\left[\psi_R^{n+1}(L-1) - \psi_R^n(L)\right] \tag{44}$$

for the real part, and,

$$\psi_I^{n+1/2}(L) = \psi_I^{n-1/2}(L-1) + r\left[\psi_I^{n+1/2}(L-1) - \psi_I^{n-1/2}(L)\right] \tag{45}$$

for the imaginary part, with the constant r given by,

$$r = \frac{v_p\Delta t - \Delta x}{v_p\Delta t + \Delta x}\ . \tag{46}$$

By definition, the phase velocity is $v_p = \omega/k$, where ω is the angular frequency of the wave. The dispersion relation between ω and k is given by [2]

$$\hbar k = \sqrt{2m(\hbar\omega - V)}\ . \tag{47}$$

Next, we note that the expression $\hbar\omega$ represents the total energy $E = K + V$ of the particle. Back substitution therefore yields,

$$v_p = \frac{\hbar\omega}{\sqrt{2m(\hbar\omega - V)}} = \frac{K+V}{\sqrt{2mK}}\ . \tag{48}$$

It is worthwhile to note how equations (44) and (45) are very similar to the classical Mur boundary of Maxwell's equations. The main difference, however, is that both ψ_R and ψ_I exist at the same grid point, while E and H typically are defined at half-step increments. As a result, the classical Mur ABC is only applied to the field that exists at the boundary, which is either E or H, but never both. Since both ψ_R and ψ_I exist at the boundary, the ABC must be applied to both quantities after each iteration of FDTD-Q.

Although the Mur ABC is relatively simple to implement, it suffers from several major trade-offs. The first is that performance diminishes with steep angles of incidence, which is a well-known limitation from classical FDTD. For simple simulations in one-dimension, this is generally not a concern since all waves impinge perpendicularly to the boundaries. In two or three dimensions, however, the problem is much more significant.

A second problem arises from the fact that phase velocity v_p of a quantum wave packet varies with ω. As a result, equations (44) and (45) exhibit a band-limited response. This requires the user to manually "tune" the Mur boundary around some given center frequency. It also means that wideband wave packets will exhibit significantly greater reflection than narrowband packets. For the case where $V > 0$, a local minimum actually appears in v_p at $K = V$, and the Mur ABC performs best around this value. However, for regions where the slope of v_p is very large, the ABC performance diminishes accordingly.

Despite its complex behavior, the simple Mur ABC can still perform reasonably well under practical conditions. To demonstrate, we generated a Gaussian wave packet with a mean kinetic energy of $K_0 = 500$ eV and a standard deviation of 2.0 Å. The packet was placed in a domain of $V = 0$ potential and directed against a tunable boundary centered at the variable energy K. Figure 1 shows a demonstration of this. If we neglect the slight spectral variance that comes from using a Gaussian envelope, the total remaining probability after the packet collides with the boundary is a fair measure of the reflection coefficient. As demonstrated in Fig. 2, a properly tuned boundary still provides as much as 35 dB of return loss on a Gaussian wave packet.

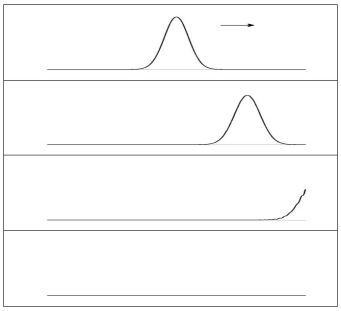

Fig. 1. Four snapshots of a Gaussian wave packet as it is absorbed by the simple Mur boundary. The mean particle energy is 500 eV and the boundary is "tuned" to the same value.

Finally, a word of warning must be noted for boundaries where $V < 0$. Under the condition $K < |V|$, ω takes on a negative value, thereby forcing v_p to be negative as well. This means the Mur ABC actually requires waves to *enter* the simulation from the boundaries instead of *leave*. As a result, numerical error quickly accumulates and destabilizes the simulation.

VI. EXAMPLE: QUANTUM TUNNELING

One of the more interesting predictions of quantum mechanics is that a particle can penetrate through a potential barrier of greater height than the particle's kinetic energy. This phenomenon, called *tunneling*, is easily

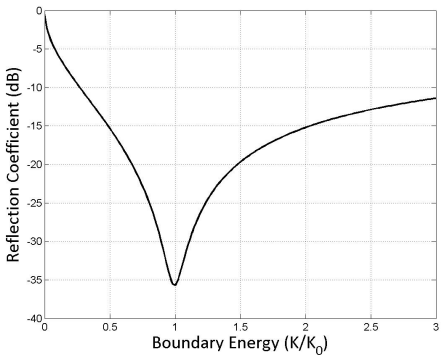

Fig. 2. Reflection coefficient of a one-dimensional Gaussian wave packet with mean kinetic energy K_0 as it reflects from a Mur absorbing boundary tuned for K.

demonstrated by FDTD-Q. It is not difficult to imagine how this could become a serious issue in the realm of modern micro-electronics. For example, the potential barrier separating the gate and source of a transistor is just such a system. If the leakage current were significantly affected by tunneling electrons, then quantum mechanics would be the only means of understanding the problem.

To begin, we define an initial value for the wave packet to represent a free particle traveling to the right, and then localize it in space by multiplying with a Gaussian envelope. For a potential barrier of thickness $2a$, the potential function is simply defined as $V(x) = V_0$, where $-a \leq x \leq a$ and V_0 is some potential energy greater than K.

Figure 3 shows a simulated demonstration of just such a system. A particle with kinetic energy of $K = 500$ eV is sent towards a potential barrier with $V_0 = 600$ eV. The grid step size is fixed at $dx = 0.005$ Å, and the barrier thickness is set to $2a = 0.25$ Å, or 50 grid points. The simulation domain consists of 3000 grid points. The figure shows four snapshots of the simulation as it progresses in time. As the particle collides with the potential barrier, some of the wave function is able to penetrate through while the rest is reflected. In the end, there is a finite probability for the particle to be found on the right side of the barrier, even though the barrier is greater than the kinetic energy of the particle.

A useful metric for characterizing a system such as this is the transmission coefficient T, which is defined as the probability that an incident particle will tunnel through the barrier. This is calculated by integrating ρ along all points to the right of the boundary and then dividing by the total probability of the system,

$$T = \frac{\int_a^\infty \rho(x)dx}{\int_{-\infty}^\infty \rho(x)dx} \ . \tag{49}$$

Note that if the wave packet is properly normalized, the denominator is identically 1. The result of this computation is a value of $T = 0.1701$, which is only 1.5% of error from its theoretical value of 0.1676 (see equation (6.14) in [8]).

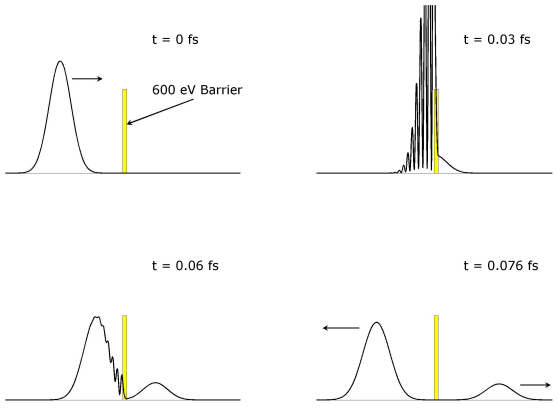

Fig. 3. Snapshots of a wave packet ρ as it collides with a potential barrier. The particle has a kinetic energy of 500 eV and the potential barrier is 600 eV. The thickness of the barrier is only 0.25 Å (50 grid points), so some of the probability penetrates to the other side.

VII. PROBABILITY CURRENT SOURCES

A useful area of research that has yet to be explored is the idea of probability sources. To date, simulations involving FDTD-Q have always required an initial-valued wave function to be pre-inserted into the domain at $t = 0$. If one is willing to forgo conservation and normalization of probability, then it is possible to inject probability into a simulation domain via probability "currents." Physically, the situation is analogous to the way electric currents radiate new electric fields. The benefit of such currents would be the potential to generate a true plane wave of probability, and would greatly facilitate the measurement of scattering parameters with complex potentials.

Mathematically, the injection of probability into a simulation domain can be achieved by simply introducing a source term into the Schrödinger equation. This is analogous to the use of "soft" current sources in the classical Maxwellian FDTD. Thus, if we define the complex-valued injection current $J(\mathbf{r},t) = J_R(\mathbf{r},t) + jJ_I(\mathbf{r},t)$ to represent a source of new probability, then equation (1) can be modified as,

$$j\hbar\frac{\partial\psi(\mathbf{r},t)}{\partial t} = -\frac{\hbar^2}{2m}\nabla^2\psi(\mathbf{r},t) + V(\mathbf{r})\psi(\mathbf{r},t) + J(\mathbf{r},t) \ . \tag{50}$$

After following the derivation through to the update equations, the only difference will be the addition of source terms onto the ends of equations (18) and (19), or more specifically,

$$\psi_R^{n+1}(i,j,k) = \ ... \ + \ c_v J_I^{n+1/2}(i,j,k) \tag{51}$$

$$\psi_I^{n+1/2}(i,j,k) = \ ... \ - \ c_v J_R^{n}(i,j,k) \ . \tag{52}$$

Figure 4 demonstrates the injection principle by simulating a real-valued, sinusoidal current at the center of an empty domain. As can be seen, what begins as an empty region of space quickly fills with probability as the wave function propagates away from the source. Because of the high-frequency content that is inherent to any transient function, ρ exhibits some natural amount of ringing after the current is suddenly introduced, and significant ripples tend to remain even long after the transients have settled down. To lessen this effect, the current source was padded with an exponential rise time, which also reduces the amount reflection at the band-limited ABCs.

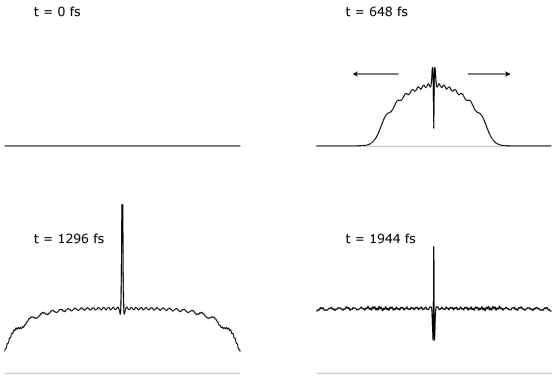

Fig. 4. Snapshots of ρ as it propagates away from the current source located in the center.

A very useful application of probability currents can be seen in Fig. 5, which demonstrates the same 600 eV barrier as that in Fig. 3. This time, instead of pre-inserting a Gaussian wave packet, a current source of the same wavenumber was inserted next to the barrier. The result is a genuine plane-wave of probability that impinges on the boundary and tunnels through. Also note the fringe pattern between the current source and the barrier. This is simply the result of interference between the forward wave and the reflected wave, and is analogous to the standing wave that develops on a transmission line with a mismatched load. The reflected wave then passes harmlessly through the current source and gets absorbed by the left boundary. The transmitted wave is likewise absorbed by the right boundary, and the steady-state result is a relatively smooth, constant amplitude to the right of the barrier.

The transmission coefficient of this system is found by first computing the average probability amplitude to the right of the boundary, and then dividing by the average amplitude that occurs in the absence of the barrier,

$$T = \frac{\int_a^\infty \rho(x)dx \mid_{barrier}}{\int_a^\infty \rho(x)dx \mid_{space}} . \tag{53}$$

Using this method, the computed value is $T = 0.160$,

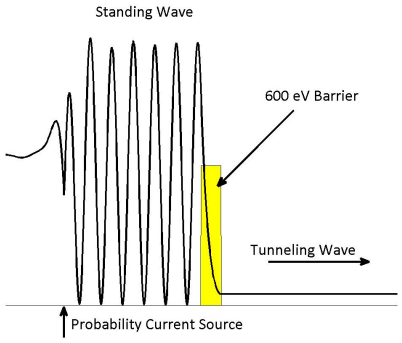

Fig. 5. A plane wave radiates away from the probability source at the left of the barrier. The wave collides with the potential barrier and partially transmits through. The rest of the wave reflects back towards the source and interferes with the forward-traveling wave, causing the fringes.

which is still only 4.8% error. The main benefit to this method, however, is that the full Gaussian packet does not need to be initialized into the grid, thereby reducing the necessary size of the simulation domain. Even when calculated on a domain of one-fifth the size (600 points), the result does not change by more than 0.1 %. Figure 6 shows the relative performance of this method against the analytical values for a varying barrier width. For a domain size of only 600 points, the mean error over the entire test range is only 3.43 %.

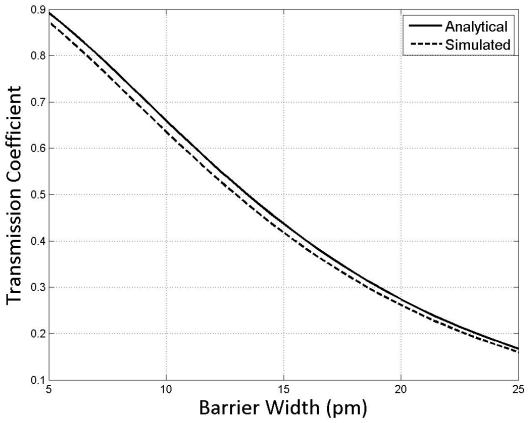

Fig. 6. Comparison of transmission coefficients for a potential barrier of varying size. Using the probability current source method, the mean error is 3.43 %.

VIII. CONCLUSIONS

This paper contains a review of FDTD-Q as applied to the time-dependent Schrödinger equation. The basic update equations have been derived in their standard form as presented in [5]. The stability criterion was rederived from a novel perspective and found to give larger stable

time steps than that given by [10]. A simple absorbing boundary condition was also formulated and shown to be effective with narrowband wave functions. Finally, the idea of probability currents was introduced for the first time and shown how it can be used to inject probability into a simulation domain.

Most of the topic of FDTD-Q is still relatively unexplored, and many interesting avenues have yet to be researched. For example, broadband absorbing boundaries have certainly been rigorously applied to various quantum simulations [2, 3, 12, 14], but none have yet to be tailored specifically to FDTD-Q in its above formulation. The idea of probability currents is also an entirely new concept, and there is still a great deal of exploration left to be done. In particular, probability currents can be used to create genuine plane waves of probability, thereby removing the need for pre-initialized wave packets in the simulation. One can also imagine other uses for current sources, such as quantum beamforming or bistatic scattering, but these topics have yet to be researched.

ACKNOWLEDGMENTS

Special thanks to Dr. Cynthia Furse for her assistance with this research and with writing this paper.

REFERENCES

[1] A. Goldberg, H. M. Schey, and J. L. Schwartz, "Computer-generated motion pictures of one-dimensional quantum mechanical transmission and reflection phenomena," *American Journal of Physics*, vol. 35, no. 3, pp. 177–186, March 1967.

[2] T. Shibata, "Absorbing boundary conditions for the finite-difference time-domain calculation of the one-dimensional Schrödinger equation," *Physical Review B*, vol. 42, no. 8, pp. 6760–6763, March 1991.

[3] J. P. Kuska, "Absorbing boundary conditions for the Schrödinger equation on finite intervals," *Physical Review B*, vol. 46, no. 8, pp. 5000 – 5003, August 1992.

[4] D. M. Sullivan, *Electromagnetic Simulation Using the FDTD Method*. New York, NY: IEEE Press, 2000.

[5] A. Soriano, E. A. Navarro, J. A. Porti, and V. Such, "Analysis of the finite difference time domain technique to solve the Schrödinger equation for quantum devices," *Journal of Applied Physics*, vol. 95, no. 12, pp. 8011 – 8018, June 2004.

[6] D. M. Sullivan and D. S. Citrin, "Determination of the eigenfunctions of arbitrary nanostructures using time-domain simulation," *Journal of Applied Physics*, vol. 91, no. 5, pp. 3219–3226, March 2002.

[7] ——, "Time-domain simulation of a universal quantum gate," *Journal of Applied Physics*, vol. 96, no. 3, pp. 1540–1546, August 2004.

[8] E. Merzbacher, *Quantum Mechanics*, 3rd ed. New York, NY: John Wiley & Sons, 1998.

[9] P. A. Tipler and R. A. Llewellyn, *Modern Physics*, 3rd ed. New York, NY: W. H. Freeman and Company, 1999.

[10] W. Dai, G. Li, R. Nassar, and S. Su, "On the stability of the FDTD method for solving a time-dependent Schrödinger equation," *Numerical Methods in Partial Differential Equations*, vol. 21, no. 6, pp. 1140–1154, April 2005.

[11] A. Arnold, M. Ehrhardt, and I. Sofronov, "Discrete transparent boundary conditions for the Schrödinger equation: Fast calculation, approximation, and stability," *Communications in Mathematical Science*, vol. 1, no. 3, pp. 501–556, 2003.

[12] Z. Xu and H. Han, "Absorbing boundary conditions for nonlinear Schrödinger equations," *Physical Review E*, vol. 74, no. 3, pp. 037 704–(1–4), March 2006.

[13] G. Mur, "Absorbing boundary conditions for the finite-difference approximation of the time-domain electromagnetic-field equations," *IEEE Transactions on Electromagnetic Compatibility*, vol. 23, no. 4, pp. 337–382, November 1981.

[14] C. Farrell and U. Leonhardt, "The perfectly matched layer in numerical simulations of nonlinear and matter waves," *Journal of Optics B: Quantum and Semiclassical Optics*, vol. 7, no. 1, pp. 1–4, January 2005.

James Nagel reveived his B.S. (04) and M.S. (06) degrees in electrical engineering from Brigham Young University in Provo, Utah. He is currently working towards a Ph.D. in electrical engineering from the University of Utah in Salt Lake City, Utah. His specialties include electromagnetics, signal processing, array theory, and FDTD simulation. He is currently conducting research in MIMO communication systems, and teaches Applied Electromagnetics.